New York State Science and Engineering Fair

Elemental Composition of Fossilized *Ceratopsidae* and *Dromaeosauridae* Teeth from the Lance Formation, Wyoming, USA

Matthew Daleo and Evan Lockwood

Introduction

The purpose of paleontology, as a science, is to advance the understanding of the ecological, geological and evolutionary patterns that took place millions of years ago. Paleontological research has evolved past the understanding of dinosaur anatomy, and has grown into a multidisciplinary science that aims to visualize and understand what life on earth was like prior to the human race (Zeigler 2014, Cooper 1958). Specifically, both biogeochemistry and chemical paleontology have seen significant development since the beginning of the 20th century (Bocherens 1997). Despite the advancement of these sciences, there are still countless gaps concerning all aspects of the interactions and developments of prehistoric life. Fossilized dinosaur teeth are some of the only existing specimen from dinosaurs that carry a similar composition of their bones as they were millions of years ago. Teeth act as the best retainers of both ecological and biological information, which ultimately makes them the most optimal specimen to use to analyze the dietary patterns, climate, environment and ecology of the world over 66 millions years ago (Bocherens 1997).

Using various methods, analyzing teeth can allow for scientists to demise conclusions about what the Earth was like as the dinosaurs were roaming it. To analyze diets, scientists reference either coprolites — which are fossilized animal stool — or fossilized organs such as gastric mills or stomachs (Zhou and Zhang 2002, Zhou et al. 2004). Other methods for identification of eating patterns are the analysis of tooth morphology/morphometry, tooth microwear, or the physical anatomy of the dinosaur (Zanno and Makovicky 2010, Samman et al. 2005, Williams et al. 2009, Mallon et al. 2013). Scientists can also study ecology or climate

using isotopic analysis of oxygen and carbon. Scientists around the world are developing new applications for teeth fossils, as some are even using them to study age, habitat, evolutionary patterns, and food resources through specific synchrotron x-ray techniques (Wang et al., 2015).

Generally, the ability to understand and conceptualize an environment that no human has ever seen would be a significant discovery in itself. Through synchrotronic methods, elemental analysis has the ability to be a driving force behind these discoveries. As so little is known about dinosaurs directly before the Cretaceous-Paleogene extinction event, studying the constituents of certain fossils add to the dynamic and growing knowledge of scientists in their quest to understand prehistoric life.

Materials and Methods

NSLS-II:

The NSLS-II (National Synchrotron Light Source II) at Brookhaven National Lab in Upton, NY is an electron storage ring of 3.0 GeV with a circumference of 792 meters that delivers photons with an average spectral brightness around 1021 ph/s. The ring has an energy range of 2-10 keV which necessitates the ring to support an electron beam of 500 mA with minimal horizontal and vertical emittance. The NSLS-II is composed of various bending magnets and insertion device sources which allows it to cover a wide range of spectra from 0.1 eV to greater than 300 keV. Currently, there are 29 beamlines in the NSLS-II with a capability of 63 at capacity. These beamlines offer various scientific or industrial services, but in this instance, it's ability to perform elemental analysis was utilized.

Sample Collection and Identification:

The samples were collected at the private Zerbst Ranch Microsite in Wyoming, USA. The microsite is the location of a prehistoric riverbed, resulting in the accumulation of diverse amounts of microfossils. With permission of the land owners, samples were collected by gloved hands and stored in zip-locked bags which were then transferred to 50 milliliter (mL) vials for transportation. The samples were identified using a basic field guide during the collection period, but then were confirmed by using extensive field guides produced for fossils found in the Hell Creek and Lance Formations. Using a trusted fossil guide for a similar locality, the specimens were identified (Brinkman 2005). Finally, the sample identification was confirmed by a seasoned fossilist (J. Hankla, Personal Communication, August 2019) Samples were labelled C1, C2, and C3 for the fossilized *Ceratopsidae* teeth, and D1, D2, and D3 for the fossilized *Dromaeosauridae* teeth.

Light Microscopic Images of Fossilized *Ceratopsidae* and *Dromaeosauridae* Teeth

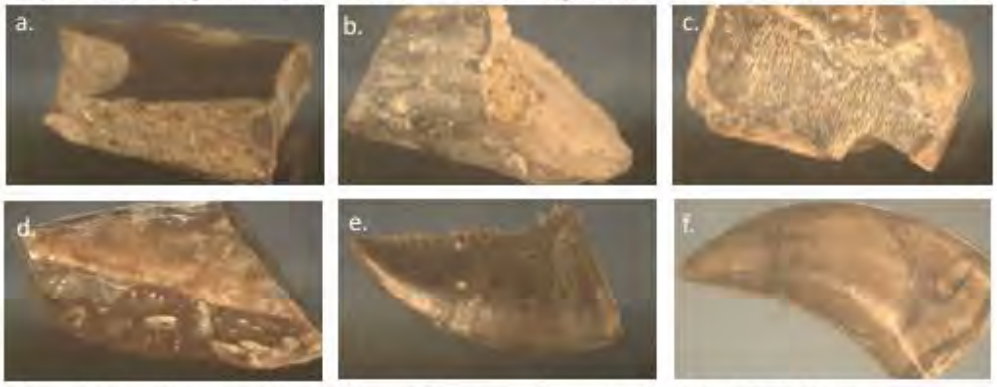

Figure 1: Light microscopy of *Ceratopsidae* and *Dromaeosauridae* teeth using a Nikon SMZ800N microscope. a. C1; b. C2; c. C3; d. D1; e. D2; f. D3.

SRX:

The Submicron-Resolution X-ray Spectroscopy Beamline (SRX 5-ID) was utilized in the analysis. The SRX 5-ID beamline has an incident x-ray beam energy of 4.65 to 25 kiloelectron volts (keV), allowing it to identify heavy elements, including most metals on the periodic table of elements. For this study, the incident energy was set to 16.5 keV, in order to see all elements with energies equal to or lower than strontium. Prior to our arrival or analysis, the beamline scientists followed standard procedure to setup and calibrate the machine. After beamline specific safety training and proper placement of TLDs, our samples were mounted. Each sample had a scanning area of 200 microns squared (μm^2) with a "Coarse Z" between 48-52 millimeters (mm), which varied between each tooth based on the topography of the sample.

Universal Sample Names

	SRX	TES	XFM
Dromaeosauridae Tooth #1 (D1)	63329 or Raptor1	raptor1	Tric1†
Dromaeosauridae Tooth #2 (D2)	63331 or Raptor2	raptor2	N/A
Dromaeosauridae Tooth #3 (D3)	63333 or Raptor3	raptor3	N/A
Ceratopsidae Tooth #1 (C1)	63335 or Tric1	tric1	Rapt1†
Ceratopsidae Tooth #2 (C2)	63337 or Tric2	tric2	N/A
Ceratopsidae Tooth #3 (C3)	63339 or Tric3	tric3	N/A
Fine Rock (FR)	63341 or FineRock	fine_rock	N/A
Coarse Rock (CR)	CoarseRock	coarse_rock	N/A

Figure 2: Samples were not given a universal name until experimentation was completed. At each beamline, data needed to be saved under a name that follows a pattern, and the researchers were advised to not repeat names across different beamlines to avoid confusion. The presence of "†" next to the sample name signifies that the sample has been cross-sectioned to allow for in-depth analysis.

The study at SRX consisted of three *Dromaeosauridae* teeth (D1, D2, D3) and three *Ceratopsidae* teeth (C1, C2, C3) and one sample of rock (FR) from the microsite that acted as a representative of the rock that the fossils were deposited in. This rock was analyzed in order to act as a negative control so we could determine whether the composition of the teeth was based upon mineral exchange or if they still contained their own composition. As shown in Figure 1 (Fig.1) , the holder has D1-D3 and FR on the left side and C1-C3 as well as CR on the right. This holder was held in the SRX hutch by a magnet on the sample holder. All samples are secured using Kapton® Tape with the flat surface facing toward the beam (Figure 3). Using Kapton® Tape is required because it does not interfere with the beamline, as it is made of a silicon adhesive, which does not interfere with SRX 5-ID's reading.

SRX Sample Holder Setup

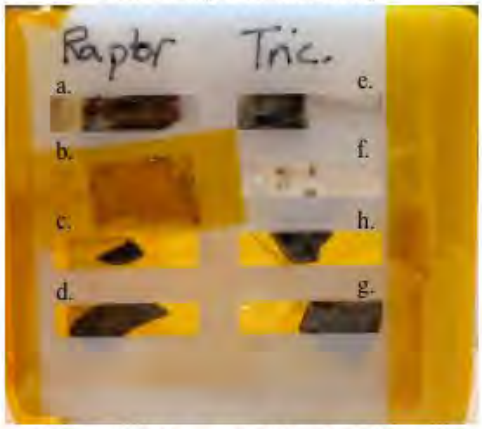

Figure 3: The sample holder setup for SRX analysis. All samples except for CR (Coarse Rock) are adhered to the holder using Kapton® Tape. The holder was provided by Brookhaven National Lab, as it is made specifically to accommodate to the design of the SRX Beamline. D: *Dromaeausauridae*; C: *Ceratopsidae.* a. D1; b. FR; c. D2; d. D3; e. C1; f. CR; g. C2; h. C3.

Eight scans were run, which were identified as 63329 (D1), 63331 (D2), 63333 (D3), 63335 (C1), 63337 (C2), 63339 (C3), 63341 (FR). The eighth scan was abandoned because the second rock sample (CR) was not prepared adequately to get coherent data from the scan. The rock that was successfully ran, 63341 or FR, was crushed using a mortar and pestle to a much finer powder compared to the more coarse, partially-ground rock and was stored in between two pieces of Kapton® Tape. Data was collected and analyzed using pyXRF software.

PyXRF:

SRX data was analyzed using PyXRF. Data from each sample was made into a Spectrum Map, individual Elemental Maps, and overlaid Red-Green-Blue (RGB) Maps, which are three elements superimposed upon each other in order to see homogeneity, heterogeneity, or other relationships between the elements in the sample. While adjusting the Spectrum Map, elements were added or deleted to align the "fit" line with the actual scan. Other peaks that were identified could have been pileup peaks, escape peaks, or scatter peaks. For pileup peaks, they were to be identified within PyXRF, but both scatter or escape peaks could not be labelled. Figures were then compared within the sample to achieve a base understanding of the type of tooth, and then compared to look for differences. The Spectrum Fit Maps for each sample were then saved to a "sum_summed" ".txt" file that was then plugged into an Excel Spreadsheet. The log of the total counts was calculated and plotted against energies (keV) of excitation. Neater spectrum graphs were produced, and we then averaged the species together for a representative of all three. This was performed for both sets of teeth, C1-C3 and D1-D3. Fr, C1-C3, and D1-D3 were superimposed upon each other in order to best compare the constituents of each. (Figure 8)

TES:

At the Tender Energy X-ray Spectroscopy Beamline (TES 8-BM) the incident x-ray beam energy is 1,000 to 5,000 electron volts (eV). The beam energy was set to 3,550 eV, which equates to 3.5 keV. The difference in units, as compared to SRX, is due to the construction of the systems at each beamline, where at SRX it used keV, and at TES, eV is employed. This beam energy allows for the beam to detect elements with a higher level of sensitivity, like P and Ca, because elements are heavier as the value for absorbance energy increases, which interferes with the sensitivity of the beam. Prior to our arrival or analysis, the beamline scientists followed standard procedure to setup and calibrate the machine. After beamline specific safety training, our samples were mounted. The scan area was set to 1000 μm^2 and the pixel size was .0118750 mm.

Seven samples were run (sample IDs: raptor1 (D1), raptor2 (D2), raptor3 (D3), tric1 (C1), tric2 (C2), tric3 (C3) and fine_rock (FR)) with the coarse rock being excluded because it could not provide any useful information at SRX in the previous analysis, due to the size and space between particles. The samples were stored in the same sample holder, but FR was placed into polypropylene bags, as the polypropylene does not interfere with the analysis on TES (Figure 4). The samples in the holder are then placed into another frame that has the capacity to support multiple specimen holders This frame was screwed into the TES hutch very carefully to avoid any contact with the beryllium screen, detectors or any other machinery within the hutch. The screen and wall of the hutch were sealed and locked, and purged of almost all of the air using an increase in the helium flow for approximately ten minutes. The air evacuation allowed for the beam to reach the sample without any interference from heavier elements commonly found in air like carbon, oxygen and nitrogen. During this process, we had to continuously watch

the concentration monitors to guarantee that the air evacuation was performing adequately. Once the hutch was evacuated of air, the analysis was allowed to begin, and data was collected. Data was analyzed using the Interactive Data Language Virtual Machine (IDL) software.

TES Sample Holder Setup

Figure 4: The sample holder setup for TES analysis. The CR (Coarse Rock) and FR (Fine Rock) and both now inside of polypropylene bags instead of Scotch ® Kapton® Tape, respectively, as the constituents of the tape interfere with the analysis. D: *Dromaeausauridae*; C: *Ceratopsidae*. a. D1 ; b. FR; c. D2; d. D3; e. C1; f. CR; g. C2; h. C3.

IDL:

The data received from the TES Beamline was processed using Interactive Data Language Virtual Machine (IDL VM) XMap Plotters. The scan resulted in one ".sav" file and nine ".isv" files per sample, each ".isv" file representing an element. The data was first opened in the ".sav" file and then each element was analyzed by opening each ".isv" file. The samples were then created into different Elemental Maps in both black and white (BW) coloring for future processing and Standard Gamma II coloring to construct color-intensity maps. The Elemental Maps were then converted to Tagged Image File Format (.tif) files. The Elemental Maps in grayscale were then run through a Python script for more accurate determinations based on the map's pixel values. Preliminary observation was done using ImageJ, a Java image observation program. The Python script used the Python Imaging Library (PIL), skimage, another

Python-based imaging library, and NumPy, a library for mathematical analysis. This Python script gave the research precise values based on a black and white scale to compare our samples to each other, rather than comparing the images to each other just by the human eye. In the grayscale, the higher value, and therefore the brighter pixel, meant that that pixel represents an area of higher intensity of the element on that sample. The Python script returned both the mean pixel value for the entire image and determined the areas on the sample with the most and least presence of a certain element and calculated those means for that area.ImageChops through PIL was used on the samples with a full map survey to create RGB images to see where elements were complementary or colocalized with each other (Figure 13).

Polishing Samples at the XFM Wet-Lab:

D1 and C1 were both planned to be symmetrically cross-sectioned in order to see past the enamel layer which would present more data regarding the initial contents of the tooth, as most chemical reactions or mineralization processes would not be able to penetrate past the enamel into the dentine layer of the teeth. D1 was too curved to be cross-sectioned vertically, so it was cross-sectioned and polished on the root and incisor ends. C1 was able to be sliced in a vertical cross section. Both of these cross-sections were performed using a diamond blade, and there was no metal involved in this process. Theoretically, carbon from a diamond blade would not affect the reading from the beamline, but if any metals were artificially placed on the tooth from the sample preparation, that would tamper with the sample. Finally, the samples were cleaned using distilled water, and the diamond saw also had a constant flow of water to avoid combustion/friction.

XFM:

The X-ray Fluorescence Microprobe (XFM 4-BM), was used to analyze C1† and D1† that were cross-sectioned and polished using a diamond blade. Prior to our arrival or analysis, the beamline scientists followed standard procedure to setup and calibrate the machine. After beamline specific safety training, our samples were mounted.The capabilities of this beamline are similar to that of the SRX beamline described before, with an incident beam ray energy capacity of 4,000 to 20,000 eV. We set our incident energy to 17996 eV, which allowed us to see all elements with energies equal or lower than 17996 eV, including most metals. Considering the element with the highest incident energy that we were looking for is strontium, we were able to see all the elements below this energy level, which is the incident energy of zirconium. This incident energy was set at this value because we wanted to see strontium and uranium in the scan. The sampling depth was about 100 μm and each point was scanned for 0.1 second. Samples were run for twelve to sixteen minutes depending on the size of the scanning area. The two teeth both had their own individual sample holder that was provided by Brookhaven National Lab. Using Kapton® Tape and two sample holders, the teeth were to be individually prepared parallel to the surface of the holder, with enough stability so that the sample could not move if slightly disturbed (Figures 5-6). To load the sample into the hutch, the beam distance was set to 95 millimeters away from the sample. To open and close the hutch, there is a multi-step protocol that ensures safety for all researchers present, which was followed exactly as instructed to us. Once the sample was set and hutch had been closed, the beam distance was decreased to 55 millimeters away. Next, we drove the beam to the four outermost corners of the sample and marked these coordinates down. Even on a sample with significant topography or angular edges, it is important to find the extremes of the expanse of the sample, even if that

meant that the beam would travel off the sample for some of the analysis. Once these coordinates for each corner had been found, we found the parameters for the sample, which told us where the beam should be directed to analyze the sample. To do this, we found the difference of the x-values, and found the length of the sample. We did the same for the y-values to find the height. We then marked the bottom left corner as the origin point (0,0), and initiated the scan from that point. XFM data was collected and analyzed in GSE MapViewer.

XFM Sample Holder Setup (C1†)

Figure 5: The sample holder setup for XFM analysis. The specimen that is pictured and labelled as "a." is C1†, after it had been vertically cross-sectioned and polished (Reference methods section to understand preparation). C1†'s polished face was faced towards the beam, and adhered using Kapton® Tape. The holder was provided by Brookhaven National Lab, as it is made specifically to accommodate to the design of the XFM Beamline. a. C1†

XFM Sample Holder Setup (D1†)

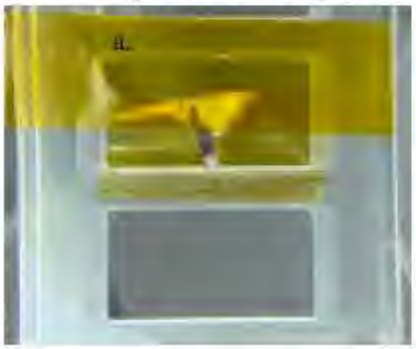

Figure 6: The sample holder setup for XFM analysis. The specimen that is pictured and labelled as "a." is D1†, which had been horizontally cross-sectioned and polished (Reference methods section to understand preparation process). D1†'s polished face was faced towards the beam, and held using Kapton® Tape. The holder was provided by Brookhaven National Lab, as it is made specifically to accommodate to the design of the XFM Beamline. a. D1†

GSE MapViewer:

In order to analyze the data allocated at the XFM beamline, we used GSE MapViewer. The was downloaded as part of the larch software package. XFM produced a single ".h5" for each sample scanned, D1 and C1. '.h5' files were imported into GSE MapViewer. This program produces Region of Interest (ROI) Maps and allows for an Elemental Map, RGB maps, Contour Plots for each Element, and correlation plots for each element detected and an X-ray

Fluorescence (XRF) Spectrum for each sample. Elements not identified in the XRF Spectrum through GSE Mapviewer (Ca, Fe, Mn, Pb, Sr, U, Y) were identified by selecting their highest and lowest channel values and then were added as a new ROI. The XRF Spectrum "x" and "y" values were exported to create graphs in Excel. These ROI Maps are maps of three elements superimposed upon each other to show the similarities and differences in the relationships of the elements, similar to the RGB Maps produced by SRX or TES data. GSE MapViewer was also utilized to produce Spectrum Maps of the teeth. The program also has the ability to analyze and produce data for specific regions of interest on the sample that can be selected by a lasso tool. Contour Plots were made using the color table RedHeat and the Elemental Map Pictures were created using the Viridis color table.

Data Analysis

SRX:

Three *Ceratopsidae* (C1-C3) and three *Dromaeosauridae* (D1-D3), as well as the Fine Rock (FR) sample, were run at the SRX beamline. The scan resulted in seven ".h5" files, but the resulting data was a truncated set due to a procedural malfunction that occured within the NSLS-II. The data that was extracted from the ".h5" files were then transformed into multiple comparative forms, including maps and graphs (Figures 7-11). Using these figures, comparisons were made. For example, RGB Maps were used to identify homogeneity, which is prevalent when there is a white color on the map, and were also used to identify colocalization by seeing patterns identified by color.

In D1, As, Tb and Fe, as well as Ca and Mn are both colocalized, respectively, and Sr is uniformly flush across the surface. In D2, Ca and Sr are homogeneously present across the surface and As, Fe, Mn, and Tb show similar patterns and are partially colocalized but not homogeneous. As for D3 Ca, Sr, Mn are flush and homogeneously present, while Fe and Tb are colocalized in a streak across the tooth horizontally. C1 shows Sr flush across the surface, with Mn only having one highly concentrated hotspot, and a total absence of As. Ca has one streak of higher intensity, but is present throughout the whole sample in high counts. Both Fe and Tb share similar localities of higher intensities hotspots. C2 followed similar patterns, with a very low presence of As detected, as well as a similar pattern of lesser concentration in a streak across the tooth for Ca and Mn both. Mn and Fe also are sporadically present, with spontaneous hotspots, and Sr and Pb are uniformly flush across the surface. Tooth C3 had Ca, Fe, Mn, and Sr flush across the surface, with no As being detected. FR had Ca, Fe, and Mn sporadically dispersed with various hotspots, while Sr showed a declining gradient down the surface. In D1, D2, and D3, Fe was always colocalized with another element, either Tb, Mn, or As. As, Fe, and Mn most commonly was found with sporadic hot spots or streaks of higher concentration, inverse to how Sr and Ca were consistently found to be uniform and flush. Most commonly, elements other than Sr were found to be most concentrated in a streak-like pattern going upwards towards the top right corner of the sample.

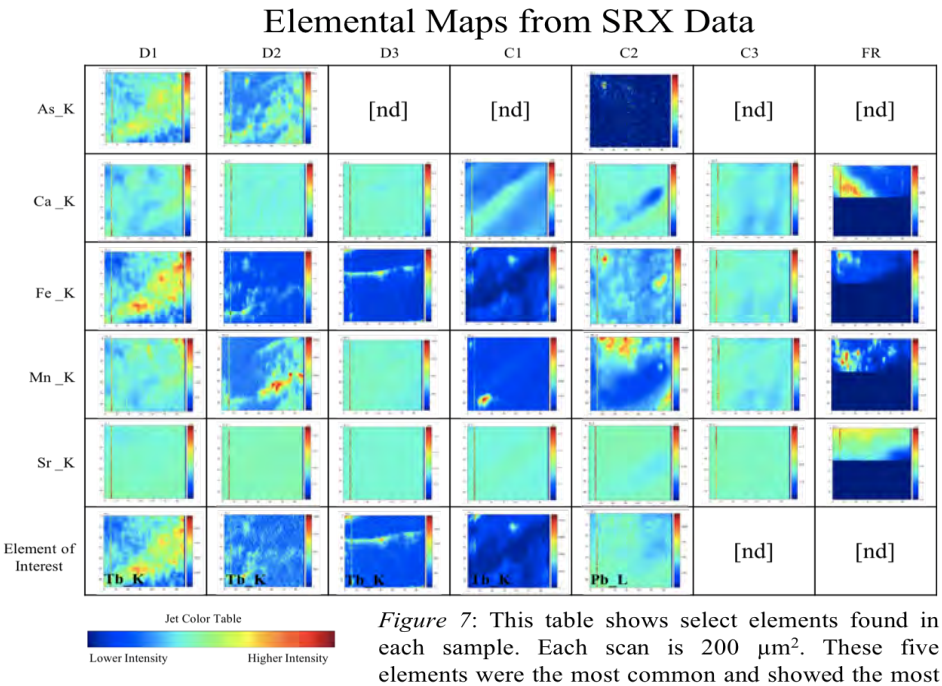

Figure 7: This table shows select elements found in each sample. Each scan is 200 μm^2. These five elements were the most common and showed the most patterns amongst the group. The "Element of Interest" section is for any other elements analyzed that followed patterns similar to that of the five selected ones, but were not present in all scans. "[nd]" – not detected in the scan.

After calibrating the Spectrum Fit graph to the Actual Scan for each data set in PyXRF, the data was saved to ".txt" files which were then turned into neater forms of the same spectra, which resembled the Elemental Spectrum provided by PyXRF, but in a neater form. Three spectra from each species were averaged and merged into one graph. This was done for C1-C3 and D1-D3. The two were superimposed upon each other, and then the graph for FR was also superimposed (Figure 8). Levels of both Ca α and Ca ß were nearly the same in the teeth, with an underwhelmingly sized peak for FR. D1-D3 had a smaller Mn peak, with larger Fe α and Fe ß peaks. For V, Ti, and Cr, the two sets of teeth were relatively equal, with FR not containing the first two, and barely any Cr. D1-D3 had discernibly greater peaks for Ni, Er, Cu, Zn, Ir, As, Br,

and Th. The rock had no peaks for Ni, Er, Cu, Ir, As, Br, or Th. The rock was the only sample to have a Pb peak, and it is a rather large one. The difference in As between the three samples may be the most significant, as FR contains none, and D1-D3 have very high counts, while C1-C3 have a moderate amount (Figure 8).

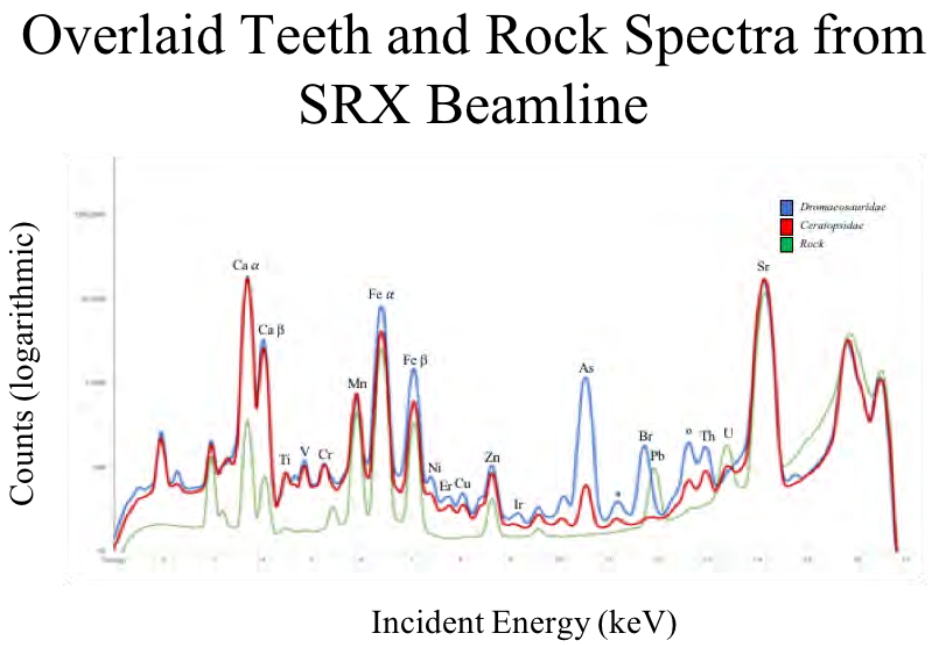

Figure 8: This graph shows three spectra overlain upon each other. The three spectra were overlaid in order to see where certain elements had higher counts or were nonexistent in the sample. (* - Ca_Ka1, Fe_Ka1; ° – Fe_Ka1, Fe_Kb1).

While spectral data confirms the presence or absence of an element, quantitative comparisons can not be derived across samples. Therefore we expressed the SRX data as a ratio of elements in a single sample, to itself. For all samples, calcium was chosen as the standard due to it similar peak size in both teeth. Total counts were divided by the Calcium counts for each sample, and ratios were plotted as a bar chart in Excel (Figures 9-11).

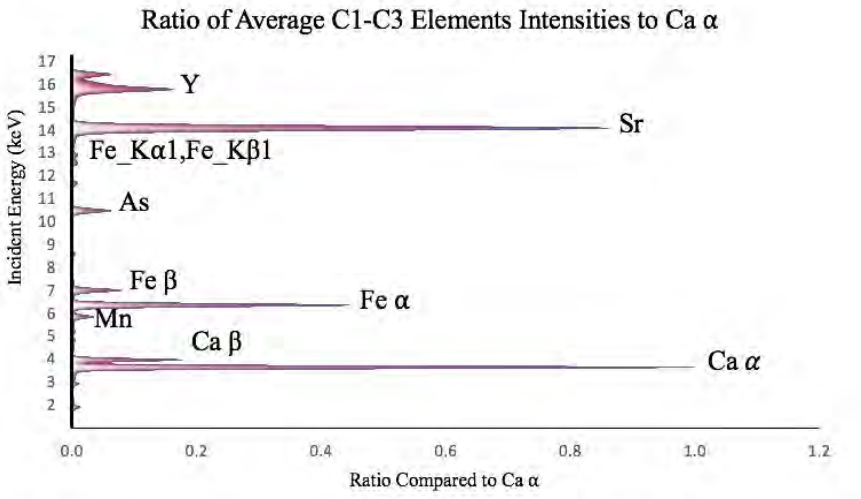

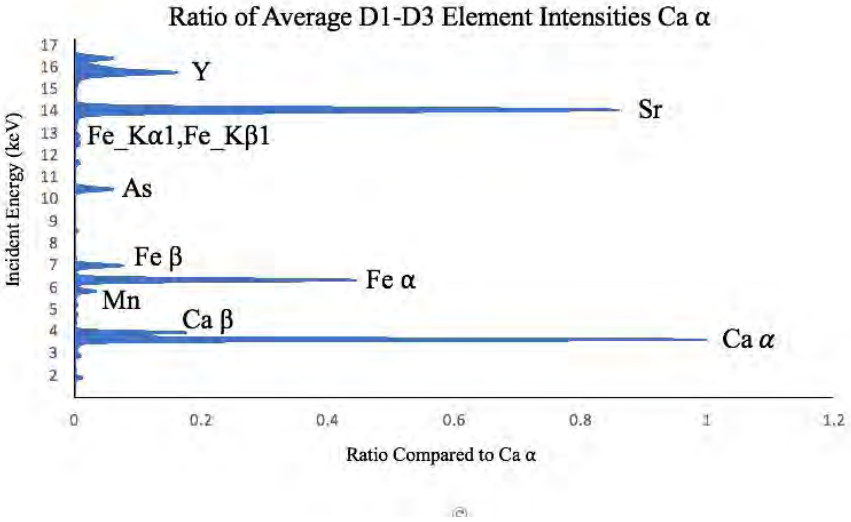

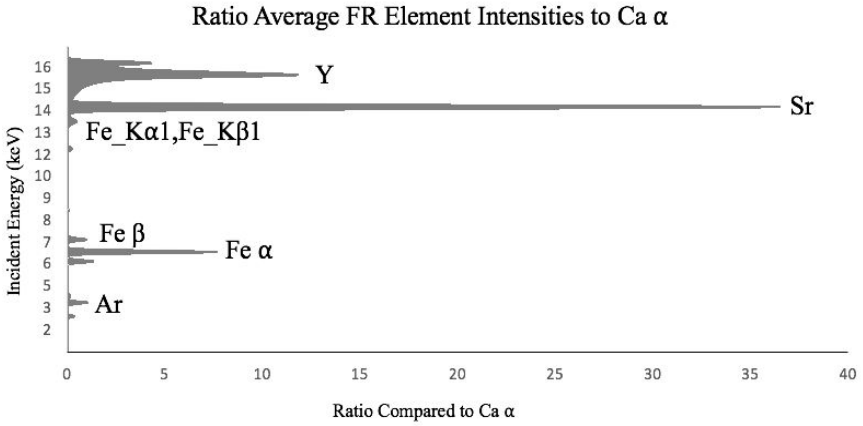

Figure 9-11: Ratios of intensity of SRX energy emissions as compared to Ca ɑ peaks for each element in the average of each species of tooth as well as FR. Intensity of emissions at each energy level was divided by the energy level for the Ca ɑ peak which was of very similar intensity among the two tooth samples. "Fe_Kɑ1,Fe_Kβ1" – pileup peak of Fe ɑ and Fe β.

TES:

Three *Ceratopsidae* and three *Dromaeosauridae*, as well as the Fine Rock (FR) sample, were run at the TES beamline. The resulting data was converted into ".tif" images and some of the images were run through the Python program that we scripted to produce multiple RGB, STD-GAMMA II, and grayscale images.

The most prominent element in all teeth is phosphorous, which was absent in the rock. P is low in crevices of all teeth. Ca was evident throughout all of the tooth samples excluding the crevices, similar to P. Ca is not detected in the rock sample. In the *Dromaeosauridae* D1, which appears to have been degraded by weathering. It showed little presence of Al and Sr_Si except in what appears to be crevices of the tooth. Ca, P, U, K were located on the surface of the tooth, and

not within the crevice. D2 and D3 showed very similar patterns to each other, which we believe is due to the pristine condition of the teeth. They both had uniform Al presence throughout the sample, as compared to D1. Uranium showed presence on the surface of both D2 and D3, and was not detected in the crevices. Sr_Si was uniformly distributed on the surface but more prominent in the crevice.

In C1, a significant contrast in Al presence, with more at the bottom of the sample where crevices are present. K and U were present at very low levels, less abundant in the crevices of the sample, and colocalized. Sr_Si is colocalized with Al, and inversely related to P.

In C2, Al and Sr_Si are heavily present in the crevices of the sample and very low presence on the surface. K, U, and Ca showed similar presence on the surface of the sample and both had lower presence in the crevices of the sample

In C3, Al has a very low presence in this sample and only have high presence in a low amount of the crevices. There was a semi-low presence of K on the surface and was mostly absent from the crevices. There was a very low presence of Sr_Si detected on the surface of this sample, with the presence peaking in numerous small depressions on the top of the sample. U and Ca where very similar in intensities, with a high presence of both on the surface and lower presence in the crevices.

FR sample show low presence in most of the elements detected. Al and P appeared in similar places, both with a very low presence. U was the most dispersed of the elements shown, but appeared in low presence. There was a very low presence of Ca throughout the sample. P had the lowest presence in the sample. Sr was highly present in the top left of the sample, where the elements appeared to be congregated.

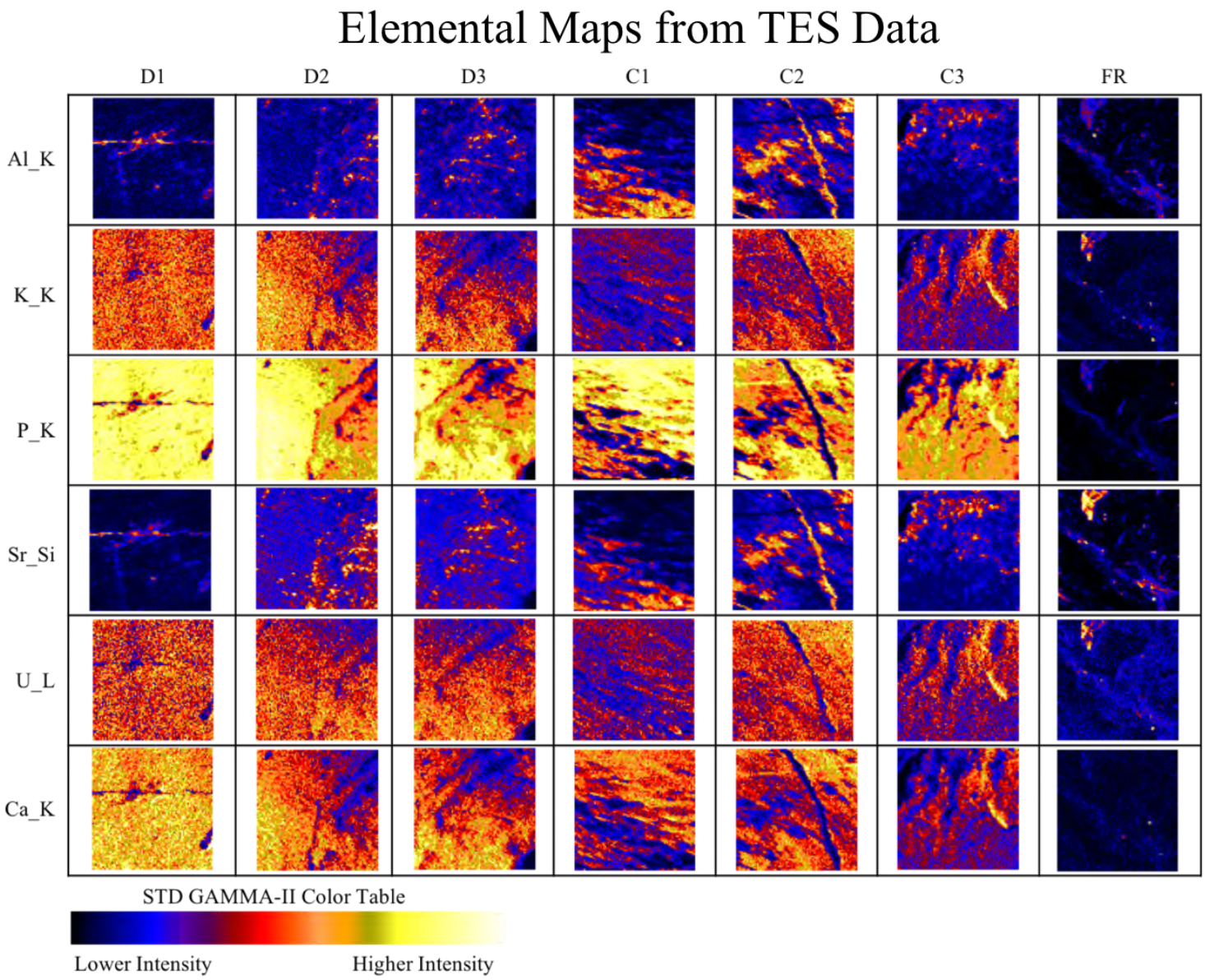

Figure 12: This table shows select elements found in each sample. Each scan is 1000 μm^2. These six elements were the most common amongst all seven scans, and showed the most patterns amongst the group.

RGB Maps from TES Data

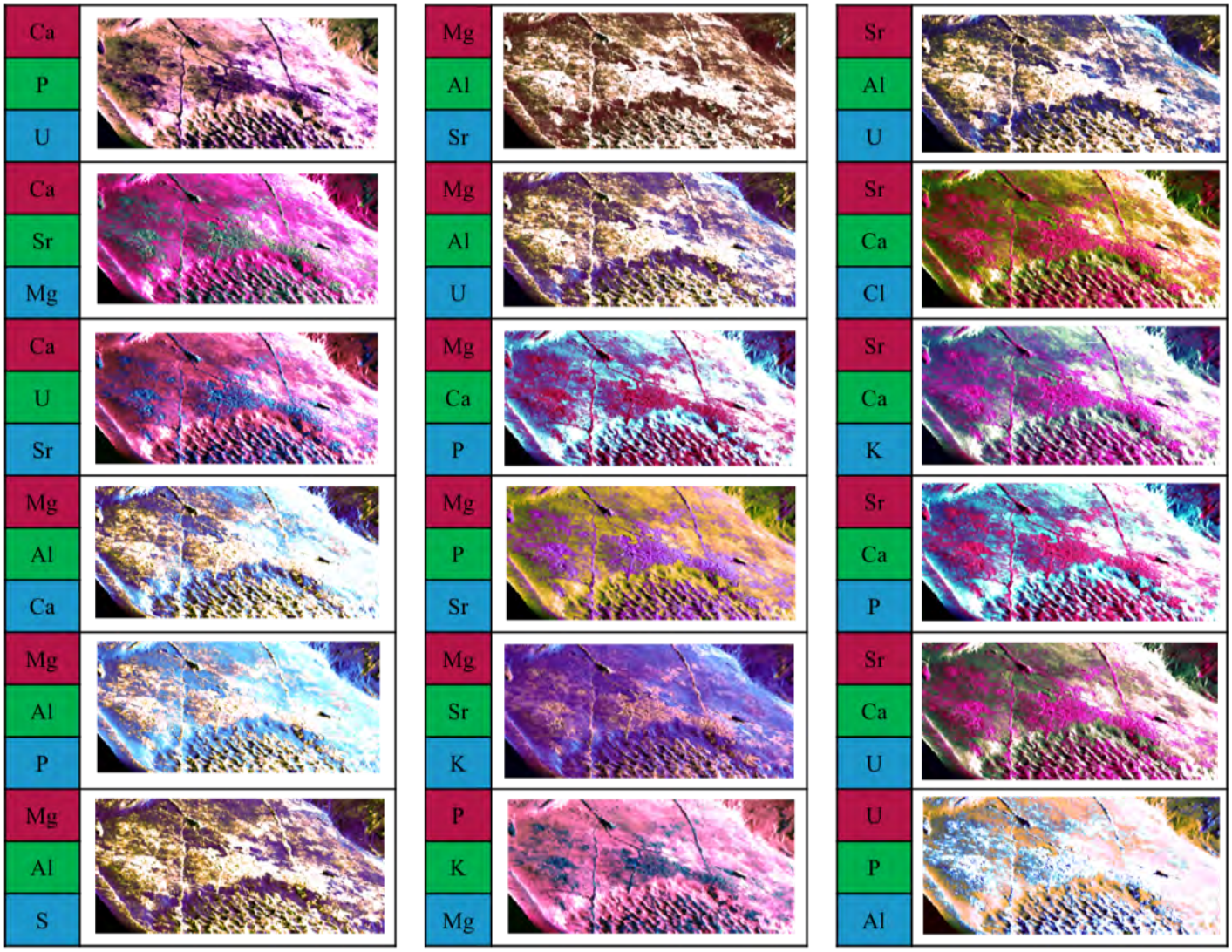

Figure 13: This figure shows the eighteen best RGB maps acquired from the TES data. RGB maps were selected by the relationships or patterns they show. The elements in the cells to the left are placed in boxes that coordinate to what color they represent in this superimposition.

XFM:

C1 and D1 were both cross-sectioned prior to experimentation on the XFM Beamline, where each sample was analyzed. Data was taken from ".h5" files and analyzed in a Larch-based GSE MapViewer program.

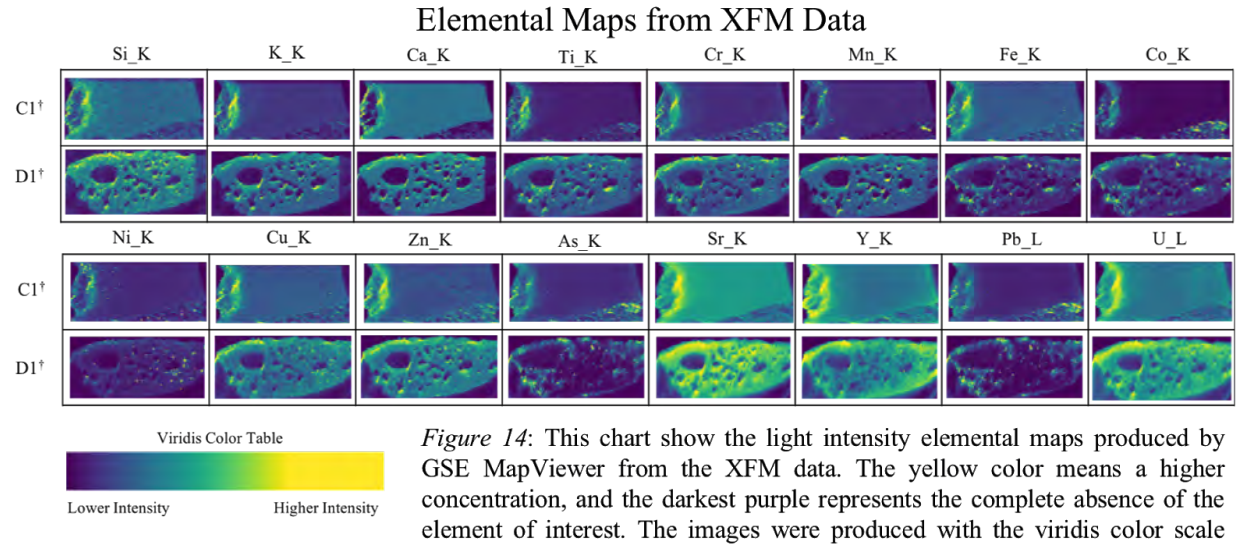

Figure 14: This chart show the light intensity elemental maps produced by GSE MapViewer from the XFM data. The yellow color means a higher concentration, and the darkest purple represents the complete absence of the element of interest. The images were produced with the viridis color scale option. Scan size varied per samples because the size of the faces of the teeth differed.

In C1, there is a low presence of K, Ti, Mn, Co, As, and Pb , while Si, Ca, Fe, Cu, and Zn showed moderately high presence, and Sr, Y, and U had the highest presence on the polished side of the tooth. The elements that appear to have the lowest presence on the polished edge of the tooth have a higher presence on the enamel. In D1 there is a low presence of Fe, Co, Ni, As, and Pb , while Si, K, Ca, Ti, Cr, Mn, Cu, and Zn showed moderately high presence, and Sr, Y, and U had the highest presence on the polished side of the tooth.

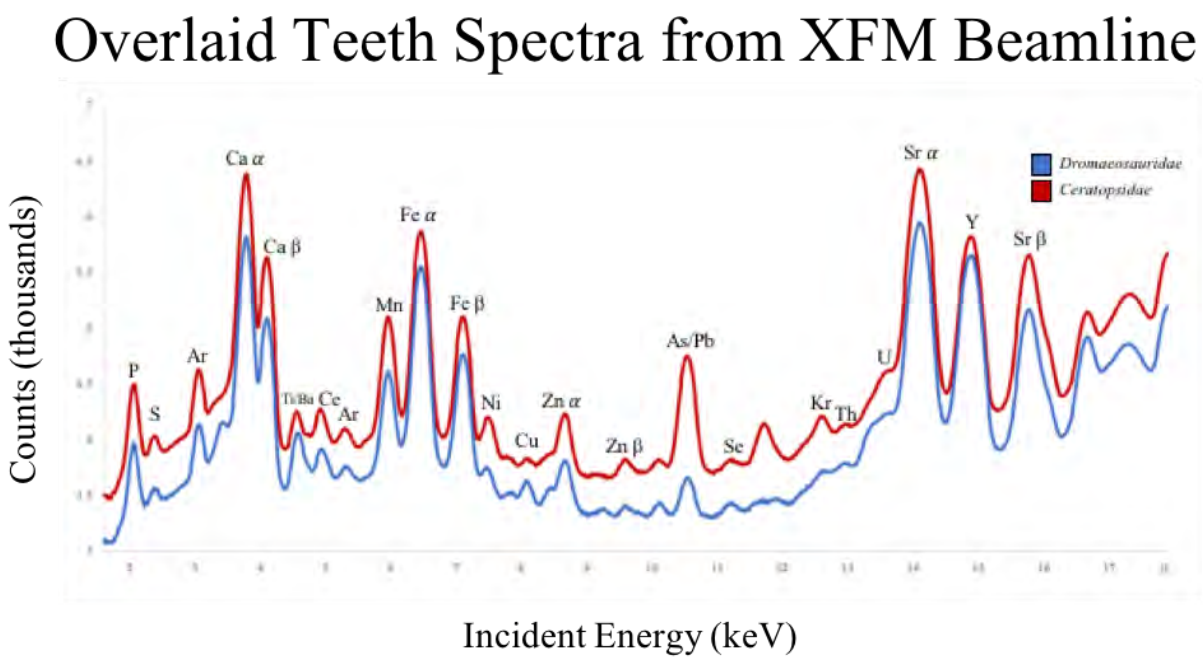

Figure 11: This graph shows two spectra overlain upon each other. The spectra of C1† and D1† were overlaid in order to see where certain elements had higher or lower counts or were nonexistent in the sample.

Discussion and Conclusion

Extensive and various studies into the story that dinosaur fossils can tell has increased science's perspective and overall understanding of the Earth's early history, and as such, it is important to continue this science as there are many discoveries needed to be made. This research can be most accurately accomplished through the use of fossilized dinosaur and prehistoric teeth, teeth are considered the best part of a specimen that are able to conserve their ecological and biological remains (Bocherens 1997).

Pb is often used as an indicator of whether or not an environmental factor has lead to a specimen's original elemental composition to be altered (Bocherens 1997). The lack of Pb throughout the samples indicate that these specimens were not contaminated by other environmental factors since their fossilization. This is further emphasized by the presence of Pb in the rock sample. However, diagenesis can change the chemical and elemental composition of bones during fossilization and proves to be an obstacle when analyzing fossil samples. These changes are dependent on surrounding environmental factors such as pH and soil compositions but is often characterized by the replacement of the Ca in the specimen's bone with Mg and Sr and increased presence of Fe, Mn, Si, and Al (Galiova et al. 2002). In Figure 8 from the SRX beamline, it is shown that both teeth samples have a high presence of Fe and Mn, but still retain a high presence of Ca. Based on the analysis at the TES beamline, Figure 12, shows that there was an absence of Mg, but high presence of Al in these samples and Figure 11 from XFM shows only a moderate presence of Si. From this it can be concluded that while diagenesis did occur in these samples, it was limited and overall did not affect the sample as the teeth continued to retain a high presence of Ca. The enamel of the teeth most likely protected the sample from significant diagenesis.

During the process of fossilization, silica and apatite have the ability change the elemental composition of fossil samples through exchanges of elements between the surrounding environment and the fossil, often resulting in minerals such as silica (silification) and apatite (Butts 2014, Newesly 1989). Silica is mainly composed of Si which has been highly present in both *Ceratopsidae* and *Dromaeosauridae* samples (Figure 12). This can be used to further influence the fact that there was a chemical change in the samples. However, silicification of

fossils is common in Paleozoic deposits, not Mesozoic, when the Cretacous is located (Butts 2014), contrasting the previous concept that silica could have changed the elemental composition of the teeth. Apatite is composed of a phosphate group (Newesly 1989), which can explain the large and mostly uniform presence of P in the fossil samples, and its absence from the rock sample. The sediment around the fossils was low in the presence of apatite and, therefore, exchange of apatite between the fossils and the sediment could have occurred. However, stronger evidence refutes this as there are elements present in the fossil samples that are completely absent from the rock (Figures 8, 11, 12). While there is evidence of apatite and silica in the rock sample, mineral exchange did not occur in the fossils. Through elemental analysis, our research has found there are unique patterns among the analyzed teeth teeth, which contained very different elements when compared to our rock sample, which was obtained from the same location as the fossil samples (Figures 8, 11, 12). This is indicative that there was an alteration in elemental composition due to biological, environmental, or ecological factors prior to fossilization, whilst the animal was alive or directly post-mortem.

There are prominent differences between the rock and dinosaur samples, such as the higher presence of As, Br, and Th in the *Dromaeosauridae*, when Br is absent, and As and Th are at a lower presence in the *Ceratopsidae* (Figure 8). Most commonly the presence of As in dinosaur fossils is an indicator that toxic arsenic helped contribute to the mass extinction of the dinosaurs (Withman et al., 2005). This arsenic is associated with large-scale volcanic eruptions that could have possibly was the result or the cause of an extinction level event. Since it is more heavily present in the *Dromaeosauridae*, this information can be channeled in a way that proves

the dinosaurs that the teeth were from, a *Dromaeosauridae* were alive during a time of severe volcanic activity.

Our study shows that elemental analysis using synchrotron technologies can provide clues as to how Cretaceous species may have lived and died in the Lance Formation, Wyoming over 65 million years ago. In the future, we hope to continue these studies using different fossilized samples and possibly doing isotopic analysis to further determine ecological conditions in which dinosaurs lived prior to, and possibly during, the catastrophic extinction event.

References

Bocherens, H. (n.d.). Encyclopedia of Dinosaurs. *Elsevier*, 107-117. Retrieved from ProQuest Multiple Databases.

Brinkman, D. (2005). An illustrated guide to the vertebrate microfossils from the Dinosaur Park Formation. *Alberta Paleontological Society*. Retrieved from ProQuest Multiple Databases.

Butts Susan H. (2014, October 1). Silification. *The Paleontological Society Paper.* Retrieved from ResearchGate

Newsely Heinrich (1989). Fossil bone apatite. *Applied Geochemistry*, 233-245. Retrieved from ScienceDirect database.

Wang, C.-C., Song, Y.-F., Song, S.-R., Ji, Q., Chiang, C.-C., Meng, Q., . . . Reisz, R. R. (2015). Evolution and Function of Dinosaur Teeth at Ultramicrostructural Level Revealed Using Synchrtron Transmission X-ray Microscopy. *Scientific Reports*, *5*(15202), 1-11.

Williams, V. S., Barnett, P. M., & Purnell, M. A. (2009). Quantitaive analysis of dental micro wear in hadrosaurid dinosaurs, and the implications for hypothesis of jaw mechanics and feeding. *PNAS*, *106*(27), 11194-11199. Retrieved from ProQuest Multiple Databases.

Witham C.S., Oppenheimer C., Horwell C.J. (2004, November 15). Volcanic ash-leachates: a review and recommendations for sampling methods. *Journal of volcanology and geothermal research*, (141), 299-326. Retrieved from ScienceDirect database.

Zanno, L. E., & Makovicky, P. J. (2011). Herbivorous eco morphology and specialization patterns in theropod dinosaur evolution. *PNAS*, *108*(1), 232-237. Retrieved from Proquest Multiple database.

Zeigler, D. (2014). *Evolution: Components and Mechanisms*. Retrieved from ScienceDirect database.

Zhou, Z., Lou, H., Hou, X., Li, G., & Li, K. (2004). Determination of arsenic in dinosaur skeleton fossils by hydride generation atomic fluorescence spectrometry. *Microchemical Journal*, (77), 29-35. Retrieved from ProQuest Multiple Databases.

Zhou, Z., & Zhang, F. (2002, July 25). A long-tailed, seed-eating bird from the Early Cretaceous of China. *letters to nature*, *418*(25), 405-409. Retrieved from ProQuest Multiple Databases.